Interaction of LDS-751 with P-Glycoprotein and Mapping of the Location of the R Drug Binding Site†

Miguel R. Lugo‡ and Frances J. Sharom*,§

Department of Molecular and Cellular Biology, University of Guelph, Guelph, Ontario, Canada N1G 2W1, and Instituto de Biología Experimental, Facultad de Ciencias, Universidad Central de Venezuela, Caracas, Venezuela

Received July 11, 2004; Revised Manuscript Received October 25, 2004

ABSTRACT: One cause of multidrug resistance is the overexpression of P-glycoprotein, a 170 kDa plasma membrane ABC transporter, which functions as an ATP-driven efflux pump with broad specificity for hydrophobic drugs, peptides, and natural products. The protein appears to interact with its substrates within the membrane environment. Previous reports suggested the existence of at least two binding sites, possibly overlapping and displaying positively cooperative interactions, termed the H and R sites for their preference for Hoechst 33342 and rhodamine 123, respectively. In this work, we have used several fluorescence approaches to characterize the molecular interaction of purified P-glycoprotein (Pgp) with the dye LDS-751, which is proposed to bind to the R site. A 50-fold enhancement of LDS-751 fluorescence indicated that the protein binding site was located in a hydrophobic environment, with a polarity lower than that of chloroform. LDS-751 bound with sub-micromolar affinity (K_d = 0.75 μM) and quenched P-glycoprotein intrinsic Trp fluorescence by 40%, suggesting that Trp emitters are probably located close to the drub-binding regions of the transporter and may interact directly with the dye. Using a FRET approach, we mapped the possible locations of the LDS-751 binding site relative to the NB domain active sites. The R site appeared to be positioned close to the membrane boundary of the cytoplasmic leaflet. The location of both H and R drug binding sites is in agreement with the idea that Pgp may operate as a drug flippase, moving substrates from the inner leaflet to the outer leaflet of the plasma membrane.

P-Glycoprotein (Pgp)[1] is a member of the ABC superfamily of membrane transporters found in organisms ranging from bacteria to humans (*1*). The multidrug transporters are believed to contribute to multidrug resistance (MDR) to chemotherapeutic drugs in some human cancers (*2*, *3*), and resistance to antibiotics and antifungal agents in microorganisms (*4*, *5*), and thus represent an important subgroup of the ABC superfamily. Eukaryotic ABC proteins are often single polypeptides characterized by an internal tandem duplication, with (typically) six transmembrane (TM) segments and one nucleotide binding (NB) domain in each half. Prokaryotic family members are more structurally diverse, and may comprise four separate subunits representing two NB and two membrane-bound domains. ATP hydrolysis at the NB domains, which are highly conserved in this protein family (*6*), drives movement of substrates across the membrane. Pgp is believed to be a highly promiscuous transporter, responsible for the altered transport across the plasma membrane of structurally diverse hydrophobic compounds, including chemotherapeutic drugs, natural products, and peptides (*7*, *8*).

Pgp appears to be different from many other membrane transporters in removing its substrates from the membrane bilayer, rather than the aqueous phase, and has been described as a "vacuum cleaner" for nonpolar compounds (*9*). The locations where drugs bind are thus believed to be within the TM domains of the protein. Cross-linking studies between Cys residues introduced into the TM regions by site-directed mutagenesis have been instrumental in pinpointing the involvement of specific TM helices in forming the binding site(s) and interacting with various drugs (*10*−*13*).

Much uncertainty has surrounded both the number of drug binding sites within Pgp and the relationship between them (*14*−*17*). Several authors have speculated that TM helices from both halves of Pgp form a single substrate-binding domain (*18*, *19*). This large, common drug-binding site would accommodate different substrates by using a combination of amino acid residues from different TM regions to form a binding site for a particular drug, according to the "substrate-induced fit" hypothesis (*20*, *21*). However, it has also been postulated that Pgp contains two drug-binding domains (*22*, *23*). Crystallographic studies have shown that soluble mul-

† This work was supported by a grant to F.J.S. from the National Cancer Institute of Canada (with funds provided by the Canadian Cancer Society) and by the Council of Scientific and Humanistic Development of Venezuela (CDCH-UCV).

* To whom correspondence should be addressed. Phone: (519) 824-4120, ext. 52247. Fax: (519) 837-1802. E-mail: fsharom@uoguelph.ca.

‡ Universidad Central de Venezuela.

§ University of Guelph.

[1] Abbreviations: ABC, ATP-binding cassette; AMP-PNP, 5′-adenylylimidodiphosphate; CHAPS, 3-[(3-cholamidopropyl)dimethylammonio]-1-propanesulfonate; DMSO, dimethyl sulfoxide; H33342, Hoechst 33342; FRET, fluorescence resonance energy transfer; GuHCl, guanidine hydrochloride; LDS-751, 2-{4-[4-(dimethylamino)phenyl]-1,3-butadienyl}-3-ethylbenzothiazolium perchlorate; MDR, multidrug resistant or resistance; MIANS, 2-(4-maleimidoanilino)naphthalene-6-sulfonic acid; NATA, *N*-acetyltryptophanamide; NB, nucleotide binding; NBD-Cl, 7-chloro-4-nitrobenz-2-oxa-1,3-diazole; Pgp, P-glycoprotein; TM, transmembrane; TNP-ATP, 2′(3′)-*O*-(2,4,6-triphenyl)-adenosine 5′-triphosphate.

10.1021/bi0485326 CCC: $30.25
Published on Web 01/11/2005

tidrug-binding proteins interact with drugs using mainly van der Waals interactions and hydrophobic stacking, rather than the precise networks of hydrogen bonds found in proteins that bind polar substrates. Multidrug-binding proteins accommodate multiple substrates by employing different side and main chain residues for different drug substrates (*24*−*26*), and it has been proposed that multidrug pumps such as Pgp use similar mechanisms (*27*, *28*).

Evidence has been obtained to support the existence within Pgp of two distinct "functional" sites for drug binding and transport, which display positive allosteric interactions. These sites can be distinguished by their different specificities, and are termed the H site and the R site, for their preferences for H33342 and colchicine, and for rhodamine 123 and anthracyclines, respectively (*29*). If a compound stimulates H33342 transport, but inhibits rhodamine 123 transport, then it is deemed to bind to the same site as rhodamine 123, i.e., the R site. On the other hand, if a compound stimulates rhodamine 123 transport, but inhibits H33342 transport, then it is deemed to bind to the same site as H33342, i.e., the H site. This simplified two-site proposal is a convenient working model for explaining stimulation of the Pgp-mediated transport of several substrates by other drugs, as for example, in the results reported by our laboratory, where hydrophobic peptides were observed to stimulate colchicine transport (*30*).

In recent years, fluorescence spectroscopy has developed into a routine experimental procedure for the study of protein−ligand interactions and intramolecular distances. In this sense, fluorescence spectroscopic approaches have been used extensively in the study of Pgp (*31*−*33*). The use of spectroscopic techniques has led to insights into its interaction with nucleotides and drugs, and both the secondary and tertiary structure of the protein. In the absence of any high-resolution structural information, fluorescence spectroscopic studies have proved to be useful in dissecting the functional architecture of Pgp (*34*−*37*). In this work, we have used fluorescence techniques to characterize the interaction of the dye LDS-751 with Pgp, and to establish the spatial relationship between its binding site (the R site) and the catalytic sites in the NB domains of the transporter.

EXPERIMENTAL PROCEDURES

Materials. 3-[(3-Cholamidopropyl)dimethylammonio]-1-propanesulfonate (CHAPS) and 7-chloro-4-nitrobenz-2-oxa-1,3-diazole (NBD-Cl) were purchased from Sigma Chemical Co. (St. Louis, MO). LDS-751 and 2-(4-maleimidoanilino)-naphthalene-6-sulfonic acid (MIANS) were obtained from Molecular Probes (Eugene, OR). Asolectin (soybean phospholipids) was obtained from Fluka (Ronkonkoma, NY).

Plasma Membrane Preparation and Pgp Purification. Plasma membrane vesicles were isolated from MDR CH^RB30 Chinese hamster ovary cells as described by Doige and Sharom (*38*), and were stored at −70 °C for no more than 3 months before being used. Plasma membrane vesicles were subjected to a two-step selective extraction with CHAPS to isolate Pgp. After treatment of the membrane vesicles with 25 mM CHAPS buffer and centrifugation, the resulting S_1 pellet was solubilized in 15 mM CHAPS buffer as described previously (*39*). Pgp was further purified from the soluble S_2 fraction by affinity chromatography on concanavalin-A-Sepharose. The final purified Pgp preparation was 90−95% pure in 50 mM Tris-HCl/0.15 M NaCl/5 mM $MgCl_2$ buffer (pH 7.5) containing 2 mM CHAPS. Protein was quantitated by the method of Bradford (*40*) for the plasma membrane and by the method of Peterson (*41*) for purified Pgp, using bovine serum albumin (crystallized and lyophilized, Sigma) as a standard.

Labeling of Purified Pgp with NBD-Cl. Labeling of the two Cys residues in the Walker A motifs of the two NB domains was carried out using previously described methods (*36*, *37*). Purified Pgp (∼250 μg/mL) was incubated with 1 mM NBD-Cl at 22 °C for 1 h in the dark. Protein labeled with NBD-Cl at both NB domains (Pgp−2NBD) was obtained by removal of unreacted NBD-Cl using a Bio-Gel P-6 gel filtration column equilibrated with 2 mM CHAPS buffer.

Fluorescence Measurements. Fluorescence spectra were recorded on a PTI Alphascan-2 spectrofluorimeter (Photon Technology International, London, ON) with the cell holder thermostated at the indicated temperature. Titration experiments were performed by adding 5 μL aliquots of a working solution of the drug to 500 μL of the protein solution in a quartz cell with a path length of 0.5 cm. The total volume of the ligand added during the titration was always 60 μL, which was 12% of the initial volume. Excitation and emission wavelengths and the bandwidth of the monochromators are indicated for each experiment. The measured fluorescence intensity was corrected for light scattering by background subtraction. When the fluorescence of the dye LDS-751 in buffer was monitored, the inner filter effect was corrected at both excitation and emission wavelengths as described elsewhere (*42*, *43*), using the expression

$$F_i^{cor} = (F_i - F_b) \times 10^{0.5(A_{\lambda ex} + A_{\lambda em})_i} \quad (1)$$

where F_i^{cor} is the corrected value of the fluorescence intensity, F_i is the experimental measured fluorescence intensity, F_b is the background fluorescence intensity caused by scattering, and $A_{\lambda ex}$ and $A_{\lambda em}$ are the absorbance of the sample at the excitation and emission wavelengths for point i of the titration, respectively. In the presence of Pgp, when either LDS-751 fluorescence or the intrinsic protein fluorescence was monitored, we corrected for the dilution of the probe (protein Trp residues or bound LDS-751) according to

$$F_i^{cor} = (F_i - F_b)\frac{V_i}{V_0} \times 10^{0.5(A_{\lambda ex} + A_{\lambda em})_i} \quad (2)$$

where V_0 is the initial volume of the sample and V_i is the volume of the sample at a given point in the titration.

Hydrophobicity of the LDS-751 Binding Site. The hydrophobicity of the LDS-751 binding site within Pgp was evaluated using the Lippert equation to describe the general solvent effect of the Stokes' shift, which is given by

$$\bar{\nu}_A - \bar{\nu}_F = \frac{2}{hc}\left(\frac{\epsilon - 1}{2\epsilon + 1} - \frac{n^2 - 1}{2n^2 + 1}\right)\frac{(\mu_E - \mu_G)^2}{a^3} + \text{constant} \quad (3)$$

In this equation, $\bar{\nu}_A$ and $\bar{\nu}_F$ are the frequency (in cm^{-1}) of the absorption and emission maxima, respectively, h is

Planck's constant (6.6256×10^{-27} J/s), c is the speed of light (2.9979×10^{10} cm/s), μ_G and μ_E are the dipole moments of the ground and excited states, respectively, ϵ is the dielectric constant, n is the refractive index of the medium, and a (in centimeters) is the radius of the cavity in which the fluorophore resides. The Lippert equation can also be expressed as

$$\bar{\nu}_A - \bar{\nu}_F = m\Delta f + \text{constant}$$

where m is the solvent sensitivity of the fluorophore and Δf is the orientation polarizability of the solvent, defined as

$$\Delta f = \left(\frac{\epsilon - 1}{2\epsilon + 1} - \frac{n^2 - 1}{2n^2 + 1}\right) \quad (4)$$

The estimation of the hydrophobicity consisted of measuring the Stokes shift of LDS-751 in several solvents of known polarizability. The Stokes shift was also determined for LDS-751 in 100 nm unilamellar vesicles of asolectin (5 mg/mL in buffer), prepared by extrusion as described previously (*39*). The solvent sensitivity (m) of the dye was then evaluated as the slope of the plot of $\bar{\nu}_A - \bar{\nu}_F$ versus Δf. The polarity of the binding site could be estimated in terms of its orientation polarizability by interpolating the Stokes shift of the dye bound to the protein.

Characterization of Binding of LDS-751 to Pgp. The affinity of LDS-751 for Pgp was estimated using two different approaches. The first method used enhancement of the fluorescence of the dye LDS-751 upon binding to the purified protein. Considering the contribution to the total fluorescence of both the free form of the dye (with a given quantum yield) and the bound form (with an increased quantum yield), the total concentration of the reagents, and using a single-site model, the following quadratic expression is obtained (*44*)

$$F_i^{cor} = Q_D\{[D]_i + 0.5(\gamma_D - 1)[(K_d + [P] + [D]_i) - \sqrt{(K_d + [P] + [D]_i)^2 - 4[P][D]_i}]\} \quad (5)$$

where Q_D (in mM^{-1}) is the molar fluorescence for the dye in the free form (in 2 mM CHAPS buffer), γ_D (dimensionless) is the fluorescence enhancement factor between the free and bound forms of the dye, [P] (in millimolar) is the total protein concentration, $[D]_i$ (in millimolar) is the total dye concentration for point i of the titration, and K_d (in millimolar) is the dissociation constant for the dye−protein complex. In absence of protein, the previous expression is reduced to

$$F_i^{cor} = Q_D[D]_i \quad (6)$$

which characterizes the fluorescence of the dye in 2 mM CHAPS buffer by means of the parameter Q_D.

In the second method, quenching of the Trp fluorescence of the protein was monitored as described previously for other Pgp substrates (*45*). The expression used in this case represents the fraction of fluorescence quenched in relation to the initial intensity, according to the expression

$$\frac{F_0^{cor} - F_i^{cor}}{F_0^{cor}} = \{0.5(1 - \gamma_P)[(K_d + [P] + [D]_i) - \sqrt{(K_d + [P] + [D]_i)^2 - 4[P][D]_i}]\}/([P]) \quad (7)$$

where F_0^{cor} is the fluorescence without the dye and γ_P (dimensionless) is the fluorescence quenching factor.

Energy Transfer from NBD to Bound LDS-751. The efficiency of resonance energy transfer (E) is typically determined using the relative fluorescence intensity of the donor in the absence (F_D) and presence (F_{DA}) of the acceptor, for a given fractional labeling with the acceptor (f_A) by means of the equation

$$E = \frac{1}{f_A}\left(1 - \frac{F_{DA}}{F_D}\right) \quad (8)$$

The FRET efficiency is related to the inverse sixth power of the distance (R) between the donor and acceptor in an isolated donor−acceptor system:

$$R = R_0(E^{-1} - 1)^{1/6} \quad (9)$$

where R_0 is the distance (in angstroms) at which the efficiency of energy transfer is 50%. R_0 can be calculated using the equation

$$R_0 = 0.211(JQ_Dk^2n^{-4})^{1/6} \quad (10)$$

where J is the spectral overlap integral between the donor and acceptor (M^{-1} cm^{-1} nm^4), Q_D is the fluorescence quantum yield of the donor, n is the refractive index of the medium, and k^2 is the orientation factor. The spectral overlap integral, J, was calculated using the integral expression

$$J = \frac{\int F_D(\lambda)\epsilon_A(\lambda)\lambda^4\, d\lambda}{\int F_D(\lambda)\, d\lambda} \quad (11)$$

where $F_D(\lambda)$ is the fluorescence emission spectrum of the donor only and $\epsilon_A(\lambda)$ (in M^{-1} cm^{-1}) is the molar extinction coefficient of the acceptor.

The fluorescence emission spectrum of the Pgp−2NBD species was recorded using excitation at 465 nm, and the spectrum of unlabeled Pgp in CHAPS buffer was subtracted. The molar absorption coefficient for LDS-751 over the wavelength range of 400−600 nm was calculated as the ratio of the absorbance at each wavelength to the absorbance at 543 nm, multiplied by the molar extinction coefficient at 543 nm (46 000 M^{-1} cm^{-1} in a nonpolar solvent, *Molecular Probes Handbook*). The value of the orientation factor, k^2, was taken to be $^2/_3$, which represents the case in which the donor and the acceptor both rotate rapidly relative to the donor fluorescence lifetime. Usually, this is the most ambiguous parameter, although differences between the true and assumed value of k^2 give known errors in the calculated distances (see later) (*46*). The quantum yield of the donor, Pgp−2NBD, was previously reported by our laboratory to be 0.023 (*35*). The refractive index of the medium between the chromophores, n, was taken to be 1.4, which is typically used for proteins in aqueous solution (*42*).

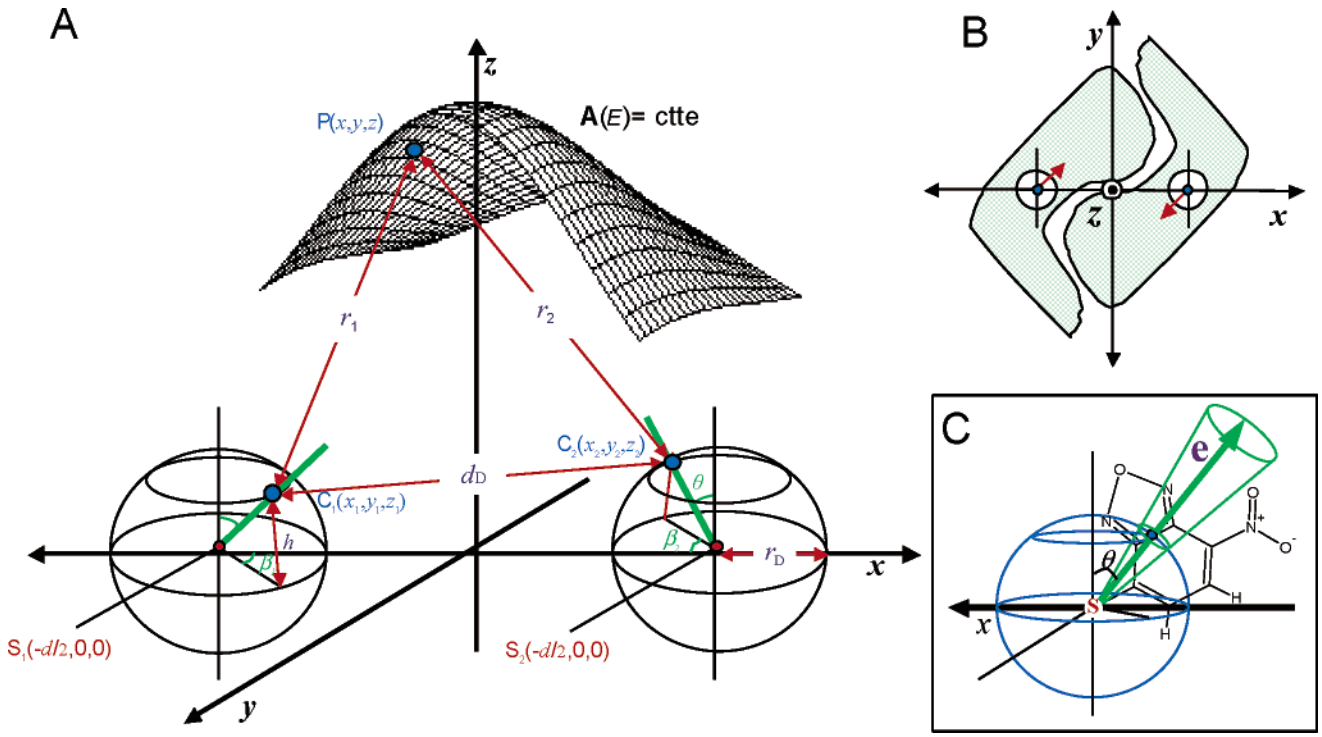

FIGURE 1: (A) Diagram showing the spatial configuration of two identical fluorescent groups centered at $C_1(x_1,y_1,z_1)$ and $C_2(x_2,y_2,z_2)$, at distances r_1 and r_2 (reduced distances), respectively, from a third fluorescent group centered at $P(x,y,z)$. Interaction of the fluorophores is by means of a FRET mechanism, and defines a surface in the space, $A(E)$, where the efficiency of the energy transferred, $E(r_1,r_2)$, is constant. In particular, for the model considered in the text, the coordinates C_1 and C_2 are indeterminate, but located on two spheres of known radius r centered at S_1 and S_2, respectively, with the relationship $\beta_2 = 180° + \beta_1$ and $\theta_1 = \theta_2 = \theta$. The distance between the C coordinates is represented by d_D and their distance from the $x-y$ plane by the height h. This model is not drawn to scale. (B) Top view of a cartoon showing the two NB domains (shaded areas) according to the structural model in which the domains face each other and are rotated by 180° (see the text). The vectors represent the orientation of the dyes within each domain. (C) Representation of an NBD group attached to an S atom. The *e*-axis links the S atom with the electronic center, $C(\theta,\beta)$, of the molecule. The cone represents the possible orientations of the *e*-axis during the lifetime of the excited state of the molecule.

Model of Energy Transfer. Let us consider the presence of two identical and distant donors, C_1 and C_2, separated from a single common acceptor, P, by distances R_1 and R_2, respectively. Considering the deactivation processes to be independent of one another, the total energy transfer efficiency of the system, according to eq 8 where $f_A = 1$, is given by

$$E = 1 - \frac{(F_{D_1A} + F_{D_2A})}{2F_D} \tag{12}$$

which can be rearranged as

$$E = (E_1 + E_2)/2 \tag{13}$$

where E_1 and E_2 are the efficiencies of transfer for each donor−acceptor pair. From Förster theory, substitution of eq 9 corresponding to each pair in eq 13 gives

$$E = \frac{1}{2}\left(\frac{{R_0}^6}{{R_0}^6 + {R_1}^6} + \frac{{R_0}^6}{{R_0}^6 + {R_2}^6}\right) \tag{14}$$

which becomes after simplifying

$$E = \frac{1}{2}\left(\frac{1}{1 + {r_1}^6} + \frac{1}{1 + {r_2}^6}\right) \tag{15}$$

where r_i is the *reduced distance* ($r_i = R_i/R_0$) between donor C_i and the acceptor. The centers of the two donors, positioned on a coordinate system defined in units of R_0 at $C_1(x_1,y_1,z_1)$ and $C_2(x_2,y_2,z_2)$, would be distances of r_1 and r_2, respectively, from the acceptor, $P(x,y,z)$, as shown in Figure 1A.

$$r_1 = \sqrt{(x - x_1)^2 + (y - y_1)^2 + (z - z_1)^2} \tag{16a}$$

$$r_2 = \sqrt{(x - x_2)^2 + (y - y_2)^2 + (z - z_2)^2} \tag{16b}$$

Equivalently, in the opposite case, where the transfer system is characterized by two identical acceptors, $C_1(x_1,y_1,z_1)$ and $C_2(x_2,y_2,z_2)$, separated from a common donor, $P(x,y,z)$, by distances r_1 and r_2, respectively, the expression of the efficiency of energy transfer would be (adapted from ref *47*)

$$E = \frac{{r_1}^6 + {r_2}^6}{{r_1}^6 + {r_2}^6 + {r_1}^6{r_2}^6} \tag{17}$$

On the basis of the geometry and expressions for the energy transfer under consideration, it is possible to calculate the surface of all possible locations for the acceptor that will explain a particular measured efficiency of transfer, E_m. To obtain the three-dimensional surface, an implicit function was defined for the efficiency $[E(r_1,r_2) = E_m]$ using either eq 15 or 17 (depending on the case being considered), in terms of distances r_1 and r_2, which are in turn functions of the floating coordinates $P(x,y,z)$ of the unique dye (the variable to be

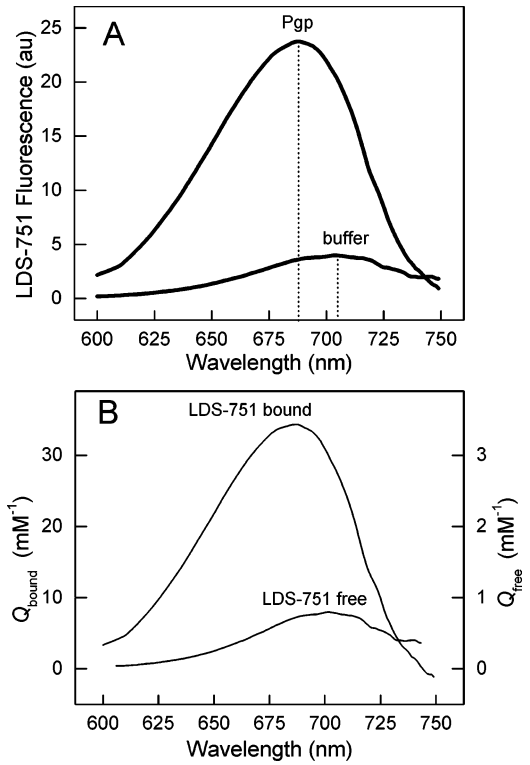

FIGURE 2: (A) Fluorescence emission spectrum of 5 μM LDS-751 in 2 mM CHAPS buffer, and in the same buffer in the presence of 100 μg/mL Pgp. Each spectrum corresponds to the difference with and without the dye (sample minus control). The dotted lines show the position of the emission maximum in each case. Excitation at 550 nm, 2 nm bandwidth, $T = 22$ °C. (B) Specific emission spectra of LDS-751. Each spectrum corresponds to the molar fluorescence for the free form of the dye in 2 mM CHAPS buffer (left axis) and bound to Pgp (right axis). The specific spectra were calculated from the emission spectra in panel A, assuming a dissociation constant K_d of 0.84 μM, according to the fit in Figure 4C.

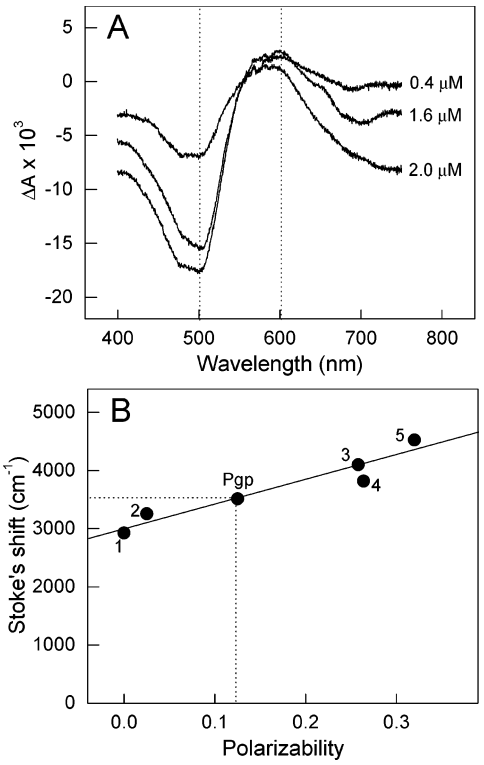

FIGURE 3: (A) Differential absorption spectra of LDS-751 at different concentrations between the condition when it is bound to Pgp (0.6 mg/mL) and free in CHAPS buffer. The difference in absorbance between the protein and the buffer in the absence of LDS-751 was established as the baseline ($\Delta A = 0$). $T = 23$ °C. (B) Stokes shift of LDS-751 in solvents with different hydrophobicities: (1) benzene, (2) 1,4-dioxane, (3) asolectin liposomes, (4) DMSO, and (5) water. LDS-751 (0.25 μM) was dissolved in the solvents, or incorporated into liposomes, and the absorption and emission spectra were measured with excitation at 550 nm. Dashed lines represent the interpolation of the Stokes shift for LDS-751 in the presence of Pgp (0.8 mg/mL) in CHAPS buffer, using the Lippert plot. $T = 22$ °C.

obtained) and the coordinates of the other attached dyes [$C_1(x_1,y_1,z_1)$ and $C_2(x_2,y_2,z_2)$].

Data Analysis. For fluorescence data acquisition and correction of the emission spectra, we used Felix 3.2 software from Photon Technology International. All calculations, manipulation, and correction of experimental data were performed in Windows Excel 2000 (Microsoft Corp.). Plotting and nonlinear curve fitting (either single or multiple) were performed using Origin 6.0 (Microcal Software Inc., Northampton, MA). For solving the implicit functions of energy transfer, we used MAPLE 9.5 (Waterloo Maple Inc., Waterloo, ON). Molecular dimensions of the fluorophores were calculated using GAUSSIAN 03 (Gaussian Inc., Pittsburgh, PA).

RESULTS

Enhancement of LDS-751 Fluorescence upon Interaction with Pgp. The fluorescent dye LDS-751 was previously reported to exhibit lipid-dependent fluorescence. LDS-751 fluorescence was enhanced 33-fold in the presence of crude soybean phosphatidylcholine liposomes, as compared with aqueous buffer (*48*). Similarly, the fluorescence intensity of LDS-751 was relatively low in 2 mM CHAPS buffer, but increased dramatically when the same buffer contained purified Pgp, as shown in Figure 2A. This increase in fluorescence indicates that the dye is in a much more nonpolar environment when it is associated with the protein, representing interaction with the drug binding sites of Pgp, which are likely located within the hydrophobic TM regions. The specificity of the interaction between the dye and the protein was demonstrated, since LDS-751 did not show significant fluorescence enhancement when Pgp was denatured using 6 M GuHCl prior to addition of the dye (Figure 4A). The enhancement of fluorescence is better appreciated when it is compared as the molar fluorescence of the dye in the free form (in buffer) and bound form (in the presence of Pgp). The specific emission spectrum of LDS-751 (Figure 2B) exhibited a shift toward shorter wavelengths (blue shift) upon binding to Pgp, presenting a maximum around 705 nm in CHAPS buffer in comparison to a value of 688 nm in the presence of the protein. This shift is characteristic of transfer of the dye into a nonpolar environment.

Characterization of the Hydrophobicity of the LDS-751 Binding Site within Pgp. The absorption spectrum of LDS-751 also depends on the properties of the solvent. LDS-751 bound to Pgp exhibited an absorption spectrum different from that of the free form in CHAPS buffer, displaying a hypochromatic region ($\Delta A < 0$) around 500 nm, and a hyperchromatic region ($\Delta A > 0$) around 600 nm (Figure 3A). The sensitivity of the LDS-751 absorbance and fluorescence spectra to the solvent polarity can be explained by the

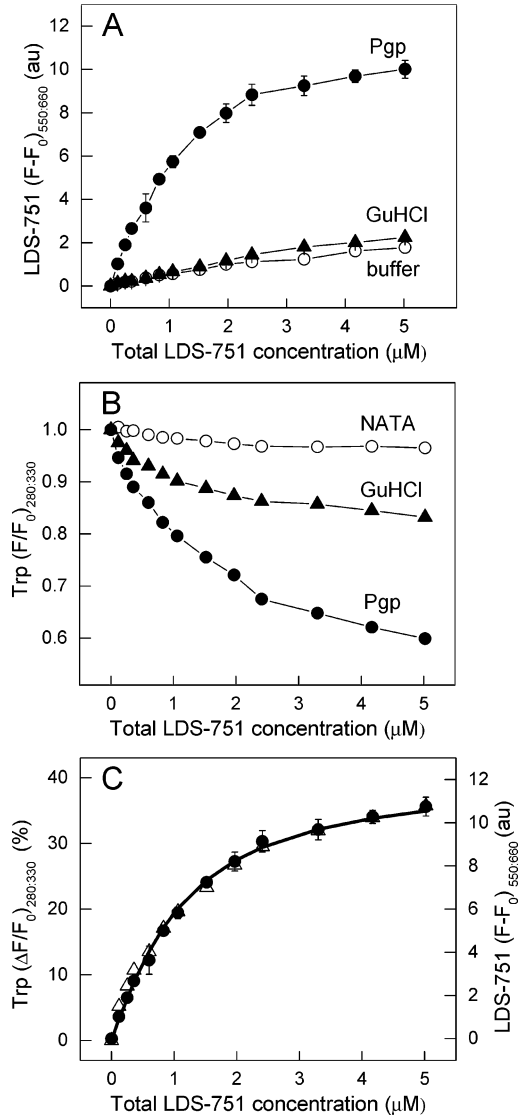

FIGURE 4: (A) Corrected fluorescence, $F - F_0$, of LDS-751 in 2 mM CHAPS buffer (○), in 100 μg/mL Pgp in 2 mM CHAPS buffer (●), and in 100 μg/mL Pgp in 6 M GuHCl (▲). The points represent the average of two or three determinations ± the standard deviation. Where errors bars are not visible, they are contained within the symbols. Excitation was at 550 nm and emission at 660 nm. (B) Fractional tryptophan fluorescence, F/F_0, of 17 μg/mL NATA in 2 mM CHAPS buffer (○), 100 μg/mL Pgp in 2 mM CHAPS buffer (●), and 100 μg/mL Pgp in 6 M GuHCl (▲). (C) Percent quenching, $\Delta F/F_0 \times 100$, of Pgp Trp fluorescence (●, left axis) and fluorescence emission intensity of LDS-751, $F - F_0$, in the presence of Pgp (△, right axis), taken from plots in panels A and B. The solid lines represent the best fit to the respective models (see the text for details). In all cases, the bandwidth was 2 nm and $T = 22$ °C.

dependence of the Stokes shift on the polarizability of the solvent, as described by the Lippert equation (eq 3). Figure 3B shows the Lippert plot for LDS-751 in solvents with different degrees of hydrophobicity, and in the presence of Pgp. The difference between the absorption and emission maxima for LDS-751 bound to Pgp was 3525 cm^{-1}, leading to an estimated polarizability Δf of 0.125, according to interpolation of the linear regression plot between both variables ($m = 4068.4$ cm^{-1}). This value of Δf is lower than those of diethyl ether (0.170) and chloroform (0.152), indicating that the LDS-751 binding site within Pgp is quite hydrophobic in nature. Indeed, the binding site for the dye is considerably more nonpolar than the interior of asolectin bilayers (see Figure 3B). This is in agreement with the observation of Shapiro and Ling that the fluorescence enhancement of LDS-751 in asolectin bilayers is only 33-fold (*48*), whereas it is 50-fold when bound to the transporter (see below).

Characterization of the Binding of LDS-751 to Pgp. One approach to studying the properties of the binding of LDS-751 to Pgp is to take advantage of changes in the fluorescence properties of the dye once bound, as previously described for other substrates (*37*, *49*). When a solution of Pgp was titrated with LDS-751, the fluorescence displayed a concentration-dependent saturable curve (Figure 4A, top plot). The fluorescence intensity increased significantly at low concentrations of the dye (less than ~2 μM) while appearing almost parallel to the buffer control at higher concentrations. Titration of the buffer with the dye led to the molar fluorescence of the free form (eq 6) at 660 nm [$Q_D = 388.8$ μM^{-1} ($R^2 = 0.986$), which was used as a fixed parameter for fitting of the titration data in the presence of Pgp. The titration of the protein denatured in GuHCl (Figure 4A) showed that either binding does not occur or, if it does, the "denatured" binding site does not exhibitdisplay the same nonpolar character.

For the titration of native Pgp in CHAPS buffer (Figure 4A), the fluorescence enhancement data were fitted using an expression for a single-site model ($n = 1$), considering a tightly binding system (eq 5). The nonlinear fitting was performed over three independent sets of data (12 points each) constrained to $0 < K_d < 1$ [determined from preliminary experiments and also close to $K_{1/2}$ estimated from the transport experiment reported by Shapiro and Ling (*48*)] and $\gamma_D > 1$. The searching algorithm minimized the quadratic difference, χ^2, reporting the following as best estimates: $K_d = 0.84 \pm 0.11$ μM and $\gamma_D = 49.52 \pm 2.31$. When the parameter Q_D was considered free-floating in the fitting routine, the uncertainty of the estimated parameters increased due to the correlation between them, since the searching was seed-dependent. Otherwise, the searching converged to the same final values. A 50-fold increase was obtained for the molar fluorescence, γ_D, when the dye was bound to Pgp in comparison to the free form.

Another approach used extensively for characterization of interactions of substrates and modulators is quenching of the intrinsic Trp fluorescence of Pgp upon binding. Titration of the purified protein with LDS-751 led to concentration-dependent saturable quenching of the Trp fluorescence (Figure 4B). Fitting of the quenching data to eq 7, constrained in this case to $\gamma_P < 1$, led to an estimated K_d of 0.75 ± 0.15 μM and a γ_p of 0.592 ± 0.014 (a maximum fluorescence quenching of 41% at saturation with LDS-751). Titration of denatured Pgp showed that, in this case, the interaction of the dye with the protein partially remains, although the Trp fluorescence is obviously affected to a much lesser degree. Figure 4C displays a plot showing the results of both signals (enhancement of LDS-751 fluorescence and quenching of Trp fluorescence) and the corresponding fitted curves. The relative magnitude of the uncertainty for each estimated parameter, and the overlap between the ranges for parameter K_d using both approaches, reflect the goodness of the fit and confirm that both fluorescence changes arise directly from the interaction of the dye with Pgp.

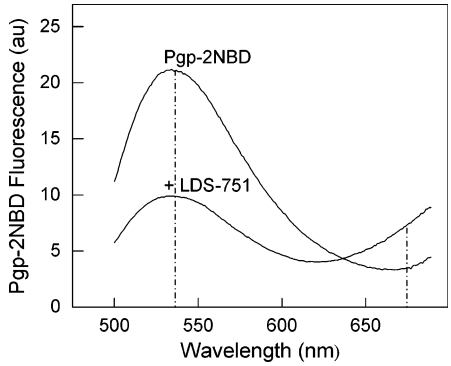

FIGURE 5: Quenching of NBD fluorescence and sensitized fluorescence emission of LDS-751 resulting from FRET. The fluorescence of Pgp−2NBD (150 μg/mL) is quenched by noncovalent binding of LDS-751 (5 μM), which in turn displays increased fluorescence due to energy transfer from the donors. The dotted lines are positioned at the emission maxima of these bands. Excitation was at 465 nm (2 nm bandwidth); the emission bandwidth was 8 nm, and $T = 22$ °C.

Energy Transfer between the LDS-751 and NBD Moieties. FRET analysis was employed to estimate the distance between the LDS-751 binding site (the putative R site) and the catalytic sites in the NB domains. To achieve this, the fluorescent dye NBD-Cl (used as the energy donor) was covalently linked to Cys residues within the Walker A motifs of the nucleotide binding folds (Cys428 and Cys1071), to give a double-labeled protein, Pgp−2NBD, as previously described (*35*, *36*). The acceptor was LDS-751 noncovalently bound to the protein. The spectral overlap integral, J, calculated according to eq 11, was calculated to be 3.4×10^{15} M^{-1} cm^{-1} nm^4 (3.4×10^{-13} M^{-1} cm^3), a value that differs by only 3.2% from that previously reported for overlap between NBD-labeled phosphatidylcholine and LDS-751 (*48*).

The fluorescence emission spectra in Figure 5 shows the quenching of the signal of the NBD probes ($\lambda_{max} = 535$ nm) by LDS-751 bound to Pgp. One explanation for this phenomenon is the existence of resonance energy transfer from the NBD moieties to the LDS-751 bound to the protein, as proposed for other drugs (*45*), although this proposal can only be validated by measuring the sensitized emission from the acceptor under excitation of the donor. It is well-known that measurement of FRET by means of the sensitization of acceptor emission is more demanding (in terms of the number of independent measurements required) than measurement by means of quenching of the donor emission (*50*). Difficulties arise if the fluorescence properties of the acceptor change for the double-labeled protein, as is the case here (see below), so this approach could not be used due to the inherent properties of the system. However, there are reasons to think that the primary means by which LDS-751 quenches the fluorescence of the NBD moieties is indeed via FRET. NBD probes are highly sensitive to the polarity of the environment (*42*). Thus, if the binding of LDS-751 produced a long-range conformational change affecting the hydrophobicity in the vicinity of the NBD probes, then a red shift would be expected for the combined emission spectrum. The spectra of Pgp−2NBD with or without LDS-751 exhibited the same emission maximum at 534−535 nm. Moreover, if the effect were differential and opposite for each NBD probe, then the maximum might be the same, but it is highly probable that

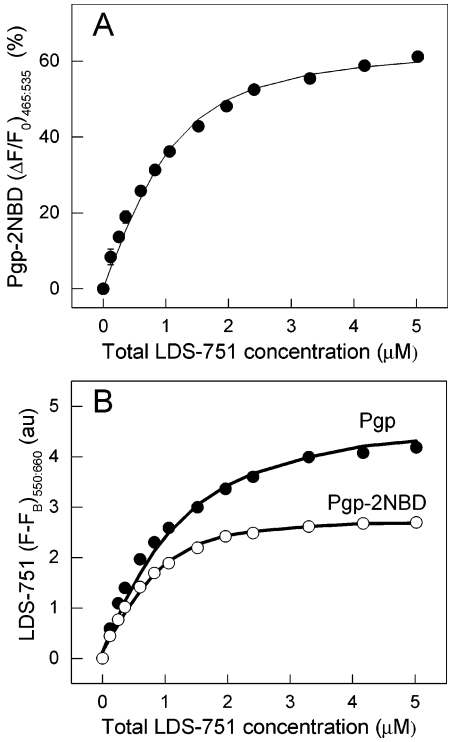

FIGURE 6: (A) Percent quenching, $\Delta F/F_0 \times 100$, of the NBD fluorescence of 150 μg/mL Pgp−2NBD during titration with LDS-751. Excitation was at 465 nm (2 nm bandwidth) and emission at 550 nm (8 nm bandwidth). (B) Enhancement of LDS-751 fluorescence, $F - F_B$, for titration of 150 μg/mL Pgp (●) and 150 μg/mL Pgp−2NBD (○) with LDS-751. Excitation was at 550 nm (2 nm bandwidth) and emission at 660 nm (8 nm bandwidth). In all cases, the solid lines represent the best fit for the binding model described in the text. $T = 22$ °C.

the shape of the emission spectrum would change. In this respect, the center of mass, CM, for each emission spectrum, defined as

$$\mathrm{CM} = \frac{\int \upsilon F(\upsilon)\, \mathrm{d}\upsilon}{\int F(\upsilon)} \tag{18}$$

is located at exactly the same wavenumber (18 513 cm^{-1}, evaluated in the range of 500−585 nm), and the bandwidths at 60% of the maximum fluorescence, $BW_{0.6}$, are essentially the same (81 and 77 nm with and without LDS-751, respectively).

The efficiency of energy transfer was measured using the relative intensity of the donor, in the absence and presence of the acceptor, for a given fractional labeling with the acceptor (eq 8). The titration of Pgp and Pgp−2NBD with LDS-751 allowed us to determine the extent of the energy transfer. Figure 6A shows the quenching of the donor NBD emission ($\lambda_{ex} = 465$ nm, $\lambda_{em} = 535$ nm) for the double-labeled protein. The fitting of these data to eq 7 allowed us to estimate the dissociation constant for LDS-751 and Pgp−2NBD ($K_d^{Pgp-2NBD} = 0.38 \pm 0.07$ μM) and the quenching factor for NBD fluorescence ($\gamma_{NBD}^{Pgp-2NBD} = 0.347 \pm 0.022$). If eq 8 is evaluated for $f_A \rightarrow 1$, the quenching factor corresponds to the relative fluorescence intensity of the donor in the presence of the acceptor ($\gamma_{NBD}^{Pgp-2NBD} = F_{DA}/F_D$), so $\Delta F_{max}/F_0$ for the fluorescence of the NBD moieties yields directly an efficiency of energy transfer (E) of 65%.

Figure 6B shows the titration of Pgp and Pgp−2NBD with LDS-751, monitoring the enhancement of LDS-751 fluorescence under direct excitation of the LDS-751 dye. Evidently, LDS-751 exhibits different binding and fluorescence behavior in each case. Using eq 5, it was possible to fit both sets of corrected data simultaneously by means of a multiple-nonlinear fitting approach, keeping Q_D (the molar fluorescence of LDS-751 free in solution) as a common (shared) parameter and constraining $K_d^{Pgp-2NBD} < K_d^{Pgp} < 1$ and $\gamma_D^{Pgp} > \gamma_D^{Pgp-2NBD} > 1$. The fitting yielded four estimated parameters: the dissociation constants for LDS-751 and Pgp ($K_d^{Pgp} = 0.70 \pm 0.12\ \mu$M) and for Pgp−2NBD ($K_d^{Pgp-2NBD} = 0.24 \pm 0.08\ \mu$M) and the fluorescence enhancement factors for the dye when bound to Pgp ($\gamma_D^{Pgp} = 45 \pm 6.25$) and to Pgp−2NBD ($\gamma_D^{Pgp-2NBD} = 25.5 \pm 1.35$). These results clearly show the influence of the covalently linked NBD moieties on the interaction of the LDS-751 with Pgp, increasing the affinity 3-fold in comparison to that of the native protein, but decreasing by half the fluorescence enhancement associated with binding. The parameters obtained for native Pgp and for Pgp−2NBD are in agreement with those established in the earlier experiments.

Spatial Interpretation of the FRET Measurements. To calculate the Förster distance for the donor−acceptor pair (NBD and LDS-751), it was necessary to obtain the quantum yield for a single Pgp−NBD moiety. For the double-labeled protein, we have determined that $Q^{Pgp-2NBD}$ equals 0.023, so the quantum yield for a single NBD group linked to Pgp ($Q^{Pgp-NBD}$) was taken to be 0.0115. The Förster distance (R_0) for this donor−acceptor pair was calculated to be 28.4 Å (eq 10), indicating that this donor−acceptor pair is able to measure distances with good accuracy in the range of 18−38 Å ($R_0 \pm 0.3R_0$).

To extract the spatial relationship between the NB domains and the LDS-751 binding site from the measured efficiency of energy transfer, it was necessary to determine the distance between both NBDs, and also to consider their relative orientation. Qu and Sharom (*36*) calculated that both Cys S atoms in the Walker A motifs were ~30 Å apart ($d = 1.05$ in terms of R_0), a value also suggested by the model of Jones and George (*51*). In the absence of any information about the orientation and mobility of the NBD probes covalently attached to the Cys S atoms, we considered in principle all possible orientations for these dyes as floating variables. This delivered two spheres centered at the positions of the Cys S atoms, at coordinates $S_1(-d/2,0,0)$ and $S_2(+d/2,0,0)$, respectively (Figure 1A), both located some distance [$r_{NBD} \approx 3.5$ Å ($0.123R_0$)] from the S atom to the center, C, of the dye (Figure 1C). In this model, the axes between the S atoms and the centers of the dye [$e_i(\theta_i,\beta_i)$] represent the time-average orientation of the molecules over a cone ($d\theta_i$ and $d\alpha_i$) of restricted motion during the excited state of the donors. Here, the e_i axes were considered isotropically oriented; that is, $0° \leq \theta_i \leq 180°$ and $0° \leq \beta_i \leq 360$. The coordinates of the centers of the molecules relative to the attachment point are defined by the angles shown, which in turn are related to the Cartesian coordinates by

$$x_i = r_{NBD} \sin\theta_i \cos\beta_i \quad (19a)$$

$$y_i = r_{NBD} \sin\theta_i \sin\beta_i \quad (19b)$$

$$z_i = r_{NBD} \cos\theta_i \quad (19c)$$

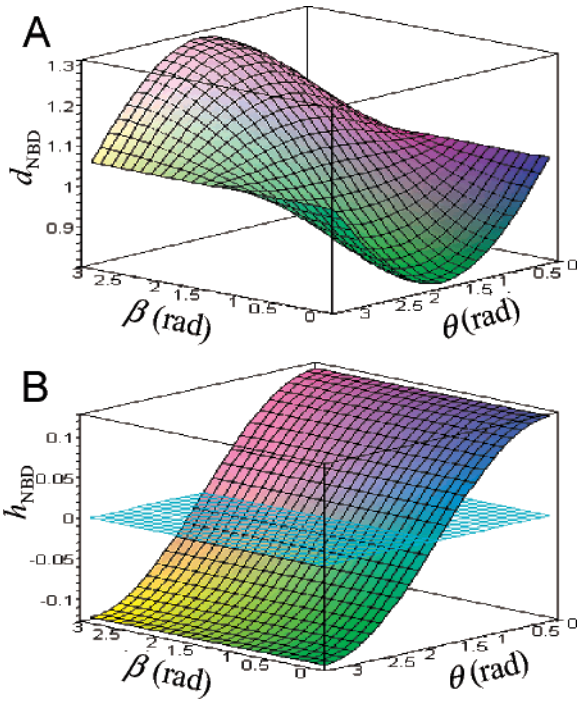

FIGURE 7: (A) Dependence of the interdonor distance on the angles β and θ defined in Figure 1. The plot shows the reduced distance between centers C_1 and C_2, d_{NBD}, when both NBD moieties ($r = r_{NBD} \approx 0.123R_0$) are oriented in the configuration indicated in the text, and attached at points S_1 and S_2 a distance d of $1.05R_0$ from each other along the x-axis. (B) Dependence of the distance of the centers of the NBD moieties from the $x-y$ plane (the height, h_{NBD}) on the angles β and θ defined in Figure 1.

In addition, we have assumed a working hypothesis about the relative orientation of the dyes according to the relative disposition of the NB domains: a mirror image in relation to the $y-z$ plane first and then to the $x-z$ plane, or *vice versa*, as depicted in Figure 1B. In spherical coordinates, this means that $\beta_2 = 180° + \beta_1$; the axes rotate in the same direction 180° out of phase. This arrangement of the NB domains is that observed in the crystal structures of BtuCD and several other NB subunits (*52*), and seems likely to be the consensus structure for the ABC protein family.

It is worth mentioning that the e-axis does not correspond to the transition moment of the dye, but a geometric axis that represents the orientation of the molecule within the NB domain. However, the orientation of the transition moments obviously remains at a constant orientation (although unknown for us) in relation to the e-axis. Despite the small size of the NBD donors in comparison to the separation of the attachment points (~30 Å), because of the sixth-power dependence of the efficiency on the distance, the estimated position of the acceptor in relation to the Cys S atoms (the reference points) is highly dependent on the distance between the centers of dyes, and therefore dependent on the relative orientation between the e-axes. The distance between both centers is a function of the angles [$d_{NBD} = f(\theta,\beta_i)$] with a minimum value d_{MIN} of $d - 2r_{NBD} \approx 23$ Å ($0.804R_0$) when the dyes are collinearly facing each other on the x-axis ($\beta_1 = 0°$ and $\beta_2 = 180°$, with $\theta = 90°$), and a maximum value d_{MAX} of $d + 2r_{NBD} \approx 37$ Å ($1.296R_0$) when the dyes are facing in the opposite direction ($\beta_1 = 180°$ and $\beta_2 = 0°$, with $\theta = 90°$) (Figure 7A). In relation to the distance of the dye centers from the $x-y$ plane, the height h from the Cys

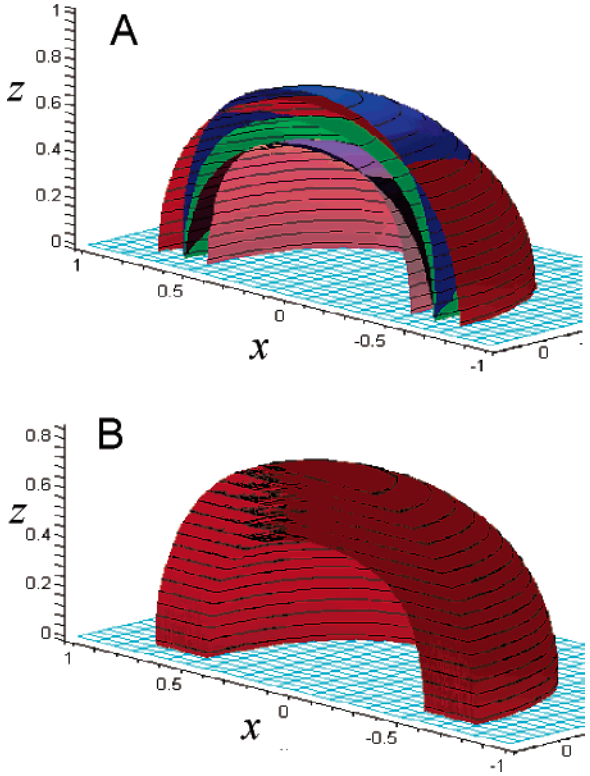

FIGURE 8: (A) *Surfaces-solution* in the upper hemisphere ($z > 0$) for the transfer system indicated in Figure 1. The surfaces correspond to the solutions of eq 15 with $E = 0.65$, $d = 30$ Å ($1.05R_0$), $r_{NBD} = 3.5$ Å ($0.123R_0$), and the coordinates of $C_i(\theta,\beta)$ as follows: $C_1(0°,\beta)$ and $C_2(0°,\beta)$, blue; $C_1(90°,0°)$ and $C_2(90°,180°)$, red; $C_1(90°,90°)$ and $C_2(90°,270°)$, green; $C_1(90°,180°)$ and $C_2(90°,0°)$, pink; $C_1(180°,\beta)$ and $C_2(180°,\beta)$, violet. (B) *Volume-solution* for the transfer system previously indicated, but ranging the angles in: $0° \leq \theta \leq 180°$ and $0° \leq \beta \leq 180°$. Axes are in units of $R_0 = 28.4$ Å.

S atoms is the same for both dyes, and only determined by the angle θ according to $h = r_{NBD} \cos \theta$ (Figure 7B).

After establishing under the working hypothesis described above the possible configurations for the center of donors, $C_1(\theta,\beta_1)$ and $C_2(\theta,\beta_2)$, we solved numerically the implicit eq 15, and were able to determine all the possible positions of the acceptor which satisfied the experimental value of transfer efficiency (E). Figure 8A shows, as an example, the surfaces-solution in the upper hemisphere ($z > 0$, where the membrane and the rest of the protein are assumed to be present, and the solution is, therefore, pertinent) for some particular configurations of the donors. Each surface comprises all the coordinates $P(x,y,z)$ that satisfy the equality $E = 0.65$ for the positions of the donors in question. The indentation of the surfaces demonstrates the dependence of the solution (the position of the acceptor) on the distance (d_{NBD}) and height (h) of the donors. The volume-solution comprises all the coordinates $P(x,y,z)$ that satisfy the equality $E = 0.65$ for at least one of all possible configurations of the pair of donors (Figure 8B). This volume represents the space where the electronic center of the acceptor (the LDS-751 dye) might be bound within Pgp, to transfer energy by a resonance mechanism of the magnitude measured, to 2NBD moieties of unknown orientation (but with a particular relationship of orientation between them) attached at two points separated by 30 Å. Figure 9 presents the curve-solution at the $x-y$ plane, as a result of positioning either two donors

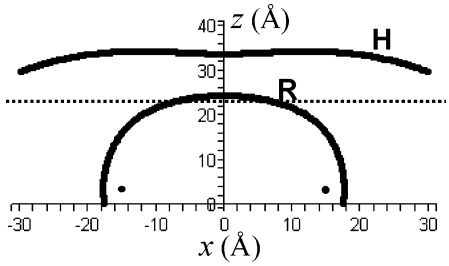

FIGURE 9: Curves-solution for the transfer system depicted in Figure 1, with the fluorescent dyes positioned at $C_1(0°,\beta)$ and $C_2(0°,\beta)$, where $d = 30$ Å and $r_{NBD} = 3.5$ Å (black dots), solving for $E = 0.60$ with $R_0 = 32.07$ Å for H33342 (taken from ref *37*) using eq 17 (curve H, putative H site) and $E = 0.65$ with $R_0 = 28.4$ Å for LDS-751 (this work) using eq 15 (curve R, putative R site). The dotted line represents the position of the inner leaflet of the bilayer according to the lower limit of 23.5 Å reported by Liu and Sharom (*35*).

or two acceptors at coordinates where $\theta = 0°$, that is, $C_1(-d/2,0,r_{NBD})$ and $C_2(+d/2,0,r_{NBD})$. For the former configuration, we used eq 15 and an E_m of 0.65, as already indicated. For the latter configuration, we used eq 17 and an E_m of 0.60, which was the energy transfer efficiency between the donor H33342 and the acceptors Pgp−2NBD from Qu et al. (*37*). Figure 9 indicates that the LDS-751 binding site, like that for H33342, is probably located in the region of the protein within the cytoplasmic leaflet of the membrane. However, the binding site is more shallowly located, close to the interfacial region of the bilayer.

DISCUSSION

Shapiro and Ling were the first to use the fluorescent DNA dye LDS-751 as a substrate for Pgp, demonstrating that the transporter removes the dye from the plasma membrane (*48*). In their transport experiments, they also showed that LDS-751 exhibited a strong lipid-dependent fluorescence, increasing its fluorescence 33-fold (at 688 nm) in the presence of phosphatidylcholine liposomes, as compared with aqueous buffer. However, this system could not be used to characterize the interaction of the dye with the protein, precisely because of the lipid-dependent fluorescence of the dye. More recently, Wang and co-workers (*53*) characterized several green tea catechins for their specific effects on the export activity of Pgp toward LDS-751 and other marker substrates. Here, working with purified Pgp in CHAPS buffer, we have demonstrated unambiguously, at the molecular level, that LDS-751 binds directly to Pgp. LDS-751 exhibited a fluorescence enhancement, γ_D, of 50-fold at 660 nm upon binding, which indicates that the dye is moved into a much more nonpolar environment. Similar behavior was reported for the lipophilic dye H33342 in its interaction with both lipid bilayers (*54*) and purified Pgp (*37*). The fact that LDS-751 did not show fluorescence enhancement when Pgp is denatured rules out the possibility of nonspecific binding to the annular lipids that remain tightly associated with the transporter after purification (*55*). The transfer of LDS-751 to a binding site within Pgp was also reflected in the spectral shift observed ($\Delta\lambda_{max} \approx -16$ nm) in comparison to aqueous buffer. This blue shift usually accompanies the increase in the quantum yield and is characteristic of transfer to a nonpolar environment, presumably in this case, to the TM regions of the protein. Simultaneously, the electronic interac-

tion of the dye with its immediate environment is perturbed upon binding, producing a shift in the absorption spectrum in comparison with the free form in water. The estimated hydrophobicity of the LDS-751 binding site within Pgp, in terms of the scale of polarity described for the orientation polarizability parameter, led to a Δf value of 0.125, indicating that this binding site is more hydrophobic than the solvents methanol (0.309), ether (0.17), and chloroform (0.152), although less hydrophobic than 1,4-dioxane (0.025). Since the substrates for Pgp are largely (although not exclusively) hydrophobic, and many have aromatic rings, the current idea is that aromatic amino acid residues may provide binding sites for these molecules via $\pi-\pi$ stacking. Pgp has a high content of aromatic residues within the TM regions compared to other ABC transporters with polar substrates, and these residues are highly conserved. Pawagi and co-workers (*20*), using molecular modeling, demonstrated that the Pgp substrate rhodamine 123 can readily intercalate between several Phe side chains in the TM helices. In addition, protein mapping studies, together with site-directed mutagenesis, have indicated that the drug and modulator binding sites are most likely within the transmembrane regions of Pgp, especially TM5, TM6, TM9, TM11, and TM12 (*56*−*58*).

Shapiro and Ling established that LDS-751 interacted preferentially with the R site, since sub-micromolar concentrations inhibited transport of rhodamine 123, while stimulating transport of H33342 (*48*). In the work presented here, we have characterized the putative R site of Pgp using the dye LDS-751, employing the same fluorescence approaches used to describe the putative H site using the dye H33342 (*37*). Here, monitoring either quenching of Pgp Trp fluorescence or enhancement of LDS-751 fluorescence upon binding, we have obtained a dissociation constant K_d of 0.70−0.85 μM for the binding of LDS-751 to purified Pgp in CHAPS buffer. This relatively low K_d value indicates that LDS-751 is an excellent probe for studying the R site, in comparison to rhodamine 123 and the anthracycline daunorubicin, whose affinities are both 15-fold lower (*32*). The K_d for LDS-751 reported here is slightly larger than the IC_{50} for rhodamine transport and the SC_{50} for H33342 transport, as reported by Shapiro and Ling (*48*), of 0.2−0.3 μM. Nevertheless, the order of magnitude of the parameters obtained by both approaches (transport and spectroscopy) is similar, sub-micromolar. Accordingly, LDS-751 fits the correlation established between these parameters (IC_{50} or SC_{50} and K_d) which has been reported for a large number of drugs and modulators (*31*, *32*).

The monophasic curve exhibited for the binding LDS-751 to Pgp, monitored by two different fluorescence signals, is in agreement with the notion of a one-site interaction for this dye (the R site). The observation of a hyperbolic binding curve is not conclusive evidence for a single binding site (the contrary is true; a nonhyperbolic curve implies $n > 1$), since different possibilities arise, as follows: (i) $n = 1$, (ii) $n > 1$, but the entire change in the fluorescence signal, ΔF_{max}, arises from only one binding site ($\Delta F_{max} = \Delta F_i$), and the remainder of the binding sites are spectroscopically silent ($\Delta F_j = 0$), or (iii) $n > 1$, but the changes in the fluorescence signal are identical for each binding site [$\Delta F(n) = n\Delta F_i$]. However, considering that the enhancement of LDS-751 fluorescence is due to the hydrophobic character of the binding site, and Pgp contains 11 Trp residues distributed nonuniformly, the last two possibilities appear to be improbable. Similar titration curves have been presented for H33342, which is proposed to interact only with the H site. The behavior of LDS-751 and H33342 differs from that of drugs such as vinblastine and verapamil (among others), where biphasic quench curves have been observed (*32*, *45*, *59*), suggesting that these particular drugs may interact with both sites with differing affinities.

With respect to the interaction of LDS-751 with the protein labeled in both NB domains with NBD moieties, the affinity of the dye for the Pgp−2NBD complex increased 2−3-fold in comparison to that of the unlabeled protein ($K_d^{Pgp-2NBD} = 0.24-0.38$ μM), as estimated by the enhancement of the LDS-751 fluorescence and quenching of the NBD groups. The enhancement itself was reduced almost 50% due to the presence of the NBD moieties; $\gamma_D = 45$ and 25 for Pgp and Pgp−2NBD, respectively. These observations possibly represent the first evidence for a change in the microenvironment of the drug binding site due to the presence of the NBD moieties in the NB domains. However, when Pgp was titrated with LDS-751 in the presence of ADP or AMP-PNP, no differences were observed (data not shown). This is also compatible with recent data reporting unaltered binding of the drugs vinblastine, doxorubicin, and H33342 to Pgp in the resting state, the ADP-bound state, and the vanadate-trapped transition state (*60*). Thus, the effect of the NBD groups on the LDS-751 interaction does not appear to correspond to the regular interaction (both structural and functional) between the NB domains and the drug binding site(s) that is presumably part of the mechanism coupling ATP hydrolysis to drug transport. In addition, ATP and AMP-PNP are still able to bind Pgp, with unchanged affinity, after covalent modification of Cys428 and Cys1071 with the dye MIANS (*39*). Therefore, the pocket within the NB domains occupied by these Cys-bound dyes is not identical to the one used by ATP (although the ATPase activity is inhibited).

Hamster Pgp (gene Pgp1) has 11 Trp residues: three in TM segments, two in extracellular loops, five in intracellular loops, and one in the C-terminal NB domain (*61*). We have suggested that only four Trp residues might be emitters: the three Trps in the TM helices and possibly Trp1105 (*45*). Here we found that the binding of LDS-751 to Pgp quenched almost 40% of the intrinsic Trp fluorescence of the protein. Quenching by resonance energy transfer from Trp to the dye must be ruled out automatically, since in contrast to another group of drugs (*45*), there is no overlap between the Pgp Trp emission spectrum and the absorption spectrum of LDS-751. Possible mechanisms of quenching include exposure of the Trps to a more polar environment (internal or external) due to a conformational change induced by LDS-751 binding, and/or a direct interaction of the drug with the Trp side chain. Collisional quenching studies and fluorescence lifetime measurements would be useful in exploring the mechanism of Trp quenching.

There is currently very little structural information available for Pgp. In particular, the location of the drug binding site(s) within Pgp has been the object of much speculation. In the absence of any high-resolution structural information, fluorescence spectroscopic studies have proved to be useful in dissecting the functional architecture of Pgp. We previously presented the first direct measurement of the location

of a drug binding site within Pgp relative to the other domains (*37*). Using a FRET approach, the H site was mapped to a location ~38 Å from the NBD probes covalently bound to the ATPase active sites, which in turn are 23−27 Å from the membrane surface (*35*). FRET estimates also indicated a maximum separation of 30 Å for the two Walker A Cys residues (*36*). Our study aimed to map the location of the R drug binding site. Since the Förster distance depends on the orientation factor and the location of the dyes involved, and the efficiency of the energy transfer is highly dependent on distance, several geometric considerations were imperative. Because of the uncertainty in the position and relative orientations of the NBD moieties within the NB domains, we considered a simplified geometry in which both Cys residues are equidistant from the plane of the membrane (assumption justified in ref *34*) and assumed that the relative position of the NBD dyes is the same for each NB domain; that is, the pocket occupied by each NBD molecule is equivalent within both NB domains. Data suggest that the Walker A motifs of the two NB domains of Pgp have practically identical local environments: (i) both NBD- and MIANS-labeled Pgp display a single-component fluorescence spectrum (*35*, *39*), (ii) a single class of fluorophores was observed during collisional quenching studies of MIANS-labeled Pgp (*34*), and (iii) ATP, AMP-PNP, and TNP-ATP binding monitored by changes in MIANS fluorescence present a single component (*34*). Additionally, the two hydrolysis events in a single catalytic cycle appear to be kinetically identical, consistent with the notion that ATP molecules are recruited randomly, and therefore, both NB domains are functional and structurally equivalent (*62*). With regard to the spatial disposition of the NB domains, they were rotated 180° relative to each other around the *z*-axis. This arrangement was suggested for Pgp by Jones and George (*51*), who rotated and manually docked one HisP monomer onto the other to produce a dimer, and also corresponds to the structure of the Rad50cd dimer (*63*) and BtuCD (*64*). It is also compatible with the orientation suggested by Loo and Clarke (*65*) from cysteine cross-linking experiments.

This hypothesis was studied using FRET analysis following a model of energy transfer in which the donors in the catalytic sites do not interact with each other, but transfer energy to a common acceptor somewhere inside the protein. The efficiency of energy transfer was set at a constant value obtained experimentally, and the transfer system (described by eqs 15, 16a, and 16b) was solved using numerical methods. The analysis yielded a graphic solution in which the reported volume contained all the possible coordinates for the center of the acceptor (LDS-751 dye) for all possible coordinates of the donors. This volume-solution was an arc centered between both donors (at the *y*-axis) and separated by ~18 Å ($0.6R_0$) vertically from the origin and ~7 Å ($0.24R_0$) in thickness. Liu and Sharom calculated that the distance of the NB domain Cys residues from the bilayer surface was 23.5−27.5 Å ($0.82-0.96R_0$) (*35*). Here, we found that the highest coordinate of the volume-solution (25 Å) is barely over the lowest limit of the position of the bilayer (23.5 Å). Thus, the binding site for LDS-751 is probably located closer to the cytoplasmic surface of the membrane than the binding site for H33342, in the interfacial region of the bilayer.

Some additional considerations can be made, as follows: (i) The range of 23.5−27.5 Å for the distance separating the NBD groups from the membrane (*35*) is an upper limit, since the effect of excluded volume was not considered in the calculation. (ii) This study was carried out in the absence of added lipids. The purified Pgp used in this work still contains ~55 tightly bound phospholipids, and displays high ATPase activity (*55*). Pgp in detergent solution and in the presence of lipid exhibited no differences in quenching of Trp residues by acrylamide, so it seems likely that protein conformation and folding, which determine accessibility to acrylamide, are the same in both cases (*45*). In addition, the binding of rhodamine 123 to Pgp in CHAPS buffer has a K_d (unpublished data) similar to that of Pgp in the presence of lipids (*60*), and similar to the K_m reported for Pgp-mediated transport (*29*). All these observations suggest that Pgp in a CHAPS solution retains its structure, and ATPase and drug binding functions. However, it is possible that the presence of a detergent might "loosen up" the protein structure, resulting in increased separation of the NB domains, as suggested previously (*36*), and might therefore affect the relative positioning of all the domains. (iii) Quenching of the NBD signal was assumed to be due entirely to FRET to LDS-751. Quenching may in fact arise from a mixed mechanism, where *E* would be slightly smaller and, therefore, the volume-solution would be located further from the donors. (iv) There is uncertainty in the k^2 factor used to calculate the Förster distance. The R_0 reported here assumed the dynamic limit ($k^2 = {}^2/_3$) for the orientation factor. However, LDS-751 is an elongated molecule (~18 Å from end to end), and it is clear that binding to Pgp causes a significant restriction in the motion of the dye. On the other hand, the NBD moiety is much smaller and is bound covalently so that free rotation of CH_2-S bonds is conceivable. It has been estimated that when the cone angle of motion of one of the probes is more than 30°, the uncertainty in the apparent donor−acceptor distance if one assumes the dynamic limit is usually less than 20% (*66*). However, for any other value from ${}^2/_3$ to 4, R_0 increases, and the distance of the volume-solution increases concomitantly.

The graphical method employed here to solve the transfer system could not map unequivocally the exact location of the R site; however, we were able to obtain reasonable evidence that the binding of the R substrate LDS-751 to Pgp (purified in a detergent solution in the absence of lipid) occurs close to the NB domains, in the cytoplasmic leaflet of the membrane. We also analyzed the energy transfer data for the dye H33342 and two NBD groups linked to Cys residues in the NB domains, reported by Qu and Sharom (*37*). Although the shape of the solution was different (at least for the configuration that was studied, $\theta = 0°$; see Figure 9), the results indicated that this drug is positioned more deeply within the cytoplasmic membrane leaflet. Figure 10 shows a three-dimensional representation of the Pgp molecule embedded in a lipid bilayer, showing the dimensions and distances between the different domains taken from various FRET and electron microscopy studies, and the curves-solution for the two substrates, H33342 and LDS-751. The projection structure of delipidated Pgp determined to ~10 Å resolution shows that the TM segments form a chamber within the membrane that appears to be open to the aqueous environment (*67*). Homology modeling of Pgp

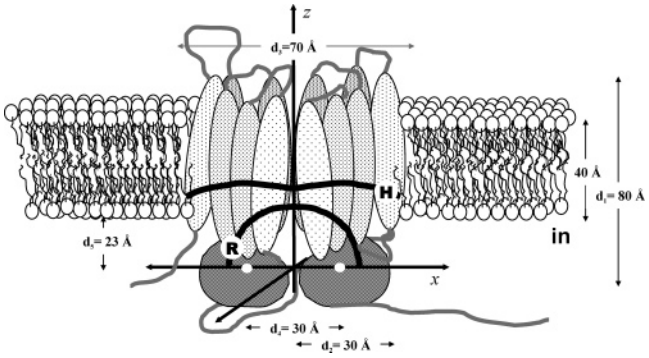

FIGURE 10: Three-dimensional cartoon representation of Pgp embedded in a lipid bilayer. The distances indicated come from crystallization studies at low resolution and FRET measurements, as follows: d_1 (taken from *ref 70*), d_2 (taken from ref *70*), d_3 (taken from refs *70* and *71*), d_4 (taken from ref *36*), and d_5 (taken from ref *35*). The cartoon also includes the curves-solution for dyes H33342 and LDS-751 taken from Figure 9. Not drawn to scale.

using the MsbA structure as a template has provided an all-atom model where there is a chamber open to both the inner bilayer leaflet and the intracellular aqueous phase (*68*). One striking feature of the Pgp chamber in this model is the presence of numerous (~20) aromatic side chains contributing to the chamber internal surface. According to the FRET data here reported, the binding of drugs could take place at the innermost end of this chamber.

Originally, the work of Shapiro and Ling (*48*, *69*) suggested that the R and H sites are probably in the cytoplasmic leaflet of the membrane, in accord with the earlier suggestion that Pgp may operate as a drug flippase (*9*). Therefore, the Pgp molecule appears to be structurally symmetrical with respect to both the catalytic sites and drug binding sites, domains that are known to be functionally interconnected. Nevertheless, this does not rule out the existence of a single common binding site or pharmacophore large enough to accommodate more than one compound, where drugs and modulators could interact with different overlapping regions.

REFERENCES

1. Schmitt, L., and Tampé, R. (2002) Structure and mechanism of ABC transporters, *Curr. Opin. Struct. Biol. 12*, 754−760.
2. Borst, P., and Oude Elferink, R. P. (2002) Mammalian ABC transporters in health and disease, *Annu. Rev. Biochem. 71*, 537−592.
3. Gottesman, M. M. (2002) Mechanisms of cancer drug resistance, *Annu. Rev. Med. 53*, 615−627.
4. Wolfger, H., Mamnun, Y. M., and Kuchler, K. (2001) Fungal ABC proteins: Pleiotropic drug resistance, stress response and cellular detoxification, *Res. Microbiol. 152*, 375−389.
5. Putman, M., Van Veen, H. W., Degener, J. E., and Konings, W. N. (2000) Antibiotic resistance: Era of the multidrug pump, *Mol. Microbiol. 36*, 772−773.
6. Holland, I. B., and Blight, M. A. (1999) ABC-ATPases, adaptable energy generators fuelling transmembrane movement of a variety of molecules in organisms from bacteria to humans, *J. Mol. Biol. 293*, 381−399.
7. Sharom, F. J. (1997) The P-glycoprotein efflux pump: How does it transport drugs? *J. Membr. Biol. 160*, 161−175.
8. Ambudkar, S. V., Dey, S., Hrycyna, C. A., Ramachandra, M., Pastan, I., and Gottesman, M. M. (1999) Biochemical, cellular, and pharmacological aspects of the multidrug transporter, *Annu. Rev. Pharmacol. Toxicol. 39*, 361−398.
9. Higgins, C. F., and Gottesman, M. M. (1992) Is the multidrug transporter a flippase? *Trends Biochem. Sci. 17*, 18−21.
10. Loo, T. W., Bartlett, M. C., and Clarke, D. M. (2004) Disulfide cross-linking analysis shows that transmembrane segments 5 and 8 of human P-glycoprotein are close together on the cytoplasmic side of the membrane, *J. Biol. Chem. 279*, 7692−7697.
11. Loo, T. W., and Clarke, D. M. (2001) Determining the dimensions of the drug-binding domain of human P-glycoprotein using thiol cross-linking compounds as molecular rulers, *J. Biol. Chem. 276*, 36877−36880.
12. Loo, T. W., and Clarke, D. M. (2000) Identification of residues within the drug-binding domain of the human multidrug resistance P-glycoprotein by cysteine-scanning mutagenesis and reaction with dibromobimane, *J. Biol. Chem. 275*, 39272−39278.
13. Loo, T. W., and Clarke, D. M. (1999) Determining the structure and mechanism of the human multidrug resistance P-glycoprotein using cysteine-scanning mutagenesis and thiol-modification techniques, *Biochim. Biophys. Acta 1461*, 315−325.
14. Ayesh, S., Shao, Y. M., and Stein, W. D. (1996) Co-operative, competitive and non-competitive interactions between modulators of P-glycoprotein, *Biochim. Biophys. Acta 1316*, 8−18.
15. Ferry, D. R., Malkhandi, P. J., Russell, M. A., and Kerr, D. J. (1995) Allosteric regulation of [^{3}H]vinblastine binding to P-glycoprotein of MCF-7 ADR cells by dexniguldipine, *Biochem. Pharmacol. 49*, 1851−1861.
16. Borgnia, M. J., Eytan, G. D., and Assaraf, Y. G. (1996) Competition of hydrophobic peptides, cytotoxic drugs, and chemosensitizers on a common P-glycoprotein pharmacophore as revealed by its ATPase activity, *J. Biol. Chem. 271*, 3163−3171.
17. Garrigos, M., Mir, L. M., and Orlowski, S. (1997) Competitive and non-competitive inhibition of the multidrug-resistance-associated P-glycoprotein ATPase-further experimental evidence for a multisite model, *Eur. J. Biochem. 244*, 664−673.
18. Morris, D. I., Greenberger, L. M., Bruggemann, E. P., Cardarelli, C., Gottesman, M. M., Pastan, I., and Seamon, K. B. (1994) Localization of the forskolin labeling sites to both halves of P-glycoprotein: Similarity of the sites labeled by forskolin and prazosin, *Mol. Pharmacol. 46*, 329−337.
19. Gottesman, M. M., and Pastan, I. (1993) Biochemistry of multidrug resistance mediated by the multidrug transporter, *Annu. Rev. Biochem. 62*, 385−427.
20. Pawagi, A. B., Wang, J., Silverman, M., Reithmeier, R. A., and Deber, C. M. (1994) Transmembrane aromatic amino acid distribution in P-glycoprotein. A functional role in broad substrate specificity, *J. Mol. Biol. 235*, 554−564.
21. Loo, T. W., and Clarke, D. M. (1999) Identification of residues in the drug-binding domain of human P-glycoprotein: Analysis of transmembrane segment 11 by cysteine-scanning mutagenesis and inhibition by dibromobimane, *J. Biol. Chem. 274*, 35388−35392.
22. Greenberger, L. M., Lisanti, C. J., Silva, J. T., and Horwitz, S. B. (1991) Domain mapping of the photoaffinity drug-binding sites in P-glycoprotein encoded by mouse mdr1b, *J. Biol. Chem. 266*, 20744−20751.
23. Garrigues, A., Loiseau, N., Delaforge, M., Ferté, J., Garrigos, M., André, F., and Orlowski, S. (2002) Characterization of two pharmacophores on the multidrug transporter P-glycoprotein, *Mol. Pharmacol. 62*, 1288−1298.
24. Zheleznova, E. E., Markham, P. N., Neyfakh, A. A., and Brennan, R. G. (1999) Structural basis of multidrug recognition by BmrR, a transcription activator of a multidrug transporter, *Cell 96*, 353−362.
25. Vazquez-Laslop, N., Zheleznova, E. E., Markham, P. N., Brennan, R. G., and Neyfakh, A. A. (2000) Recognition of multiple drugs by a single protein: A trivial solution of an old paradox, *Biochem. Soc. Trans. 28*, 517−520.
26. Schumacher, M. A., and Brennan, R. G. (2002) Structural mechanisms of multidrug recognition and regulation by bacterial multidrug transcription factors, *Mol. Microbiol. 45*, 885−893.
27. Zheleznova, E. E., Markham, P., Edgar, R., Bibi, E., Neyfakh, A. A., and Brennan, R. G. (2000) A structure-based mechanism for drug binding by multidrug transporters, *Trends Biochem. Sci. 25*, 39−43.
28. Neyfakh, A. A. (2002) Mystery of multidrug transporters: The answer can be simple, *Mol. Microbiol. 44*, 1123−1130.
29. Shapiro, A. B., and Ling, V. (1997) Positively cooperative sites for drug transport by P-glycoprotein with distinct drug specificities, *Eur. J. Biochem. 250*, 130−137.
30. Sharom, F. J., Yu, X., DiDiodato, G., and Chu, J. W. K. (1996) Synthetic hydrophobic peptides are substrates for P-glycoprotein and stimulate drug transport, *Biochem. J. 320*, 421−428.

31. Sharom, F. J., Liu, R., and Romsicki, Y. (1998) Spectroscopic and biophysical approaches for studying the structure and function of the P-glycoprotein multidrug transporter, *Biochem. Cell Biol. 76*, 695−708.
32. Sharom, F. J., Liu, R., Romsicki, Y., and Lu, P. (1999) Insights into the structure and substrate interactions of the P-glycoprotein multidrug transporter from spectroscopic studies, *Biochim. Biophys. Acta 1461*, 327−345.
33. Sharom, F. J., Liu, R., Qu, Q., and Romsicki, Y. (2001) Exploring the structure and function of the P-glycoprotein multidrug transporter using fluorescence spectroscopic tools, *Semin. Cell Dev. Biol. 12*, 257−266.
34. Liu, R., and Sharom, F. J. (1997) Fluorescence studies on the nucleotide binding domains of the P-glycoprotein multidrug transporter, *Biochemistry 36*, 2836−2843.
35. Liu, R., and Sharom, F. J. (1998) Proximity of the nucleotide binding domains of the P-glycoprotein multidrug transporter to the membrane surface: A resonance energy transfer study, *Biochemistry 37*, 6503−6512.
36. Qu, Q., and Sharom, F. J. (2001) FRET analysis indicates that the two ATPase active sites of the P-glycoprotein multidrug transporter are closely associated, *Biochemistry 40*, 1413−1422.
37. Qu, Q., and Sharom, F. J. (2002) Proximity of bound Hoechst 33342 to the ATPase catalytic sites places the drug binding site of P-glycoprotein within the cytoplasmic membrane leaflet, *Biochemistry 41*, 4744−4752.
38. Doige, C. A., and Sharom, F. J. (1991) Strategies for the purification of P-glycoprotein from multidrug-resistant Chinese hamster ovary cells, *Protein Expression Purif. 2*, 256−265.
39. Liu, R., and Sharom, F. J. (1996) Site-directed fluorescence labeling of P-glycoprotein on cysteine residues in the nucleotide binding domains, *Biochemistry 35*, 11865−11873.
40. Bradford, M. M. (1976) A rapid and sensitive method for the quantitation of microgram quantities of protein utilizing the principle of protein-dye binding, *Anal. Biochem. 72*, 248−254.
41. Peterson, G. L. (1977) A simplification of the protein assay method of Lowry et al. which is more generally applicable, *Anal. Biochem. 83*, 346−356.
42. Lakowicz, J. R. (1999) *Principles of Fluorescence Spectroscopy*, Kluwer Academic Publishers, New York.
43. Birdsall, B., King, R. W., Wheeler, M. R., Lewis, C. A., Jr., Goode, S. R., Dunlap, R. B., and Roberts, G. C. (1983) Correction for light absorption in fluorescence studies of protein−ligand interactions, *Anal. Biochem. 132*, 353−361.
44. Kubala, M., Plasek, J., and Amler, E. (2003) Limitations in linearized analyses of binding equilibria: Binding of TNP-ATP to the H4−H5 loop of Na/K-ATPase, *Eur. Biophys. J. 32*, 363−369.
45. Liu, R., Siemiarczuk, A., and Sharom, F. J. (2000) Intrinsic fluorescence of the P-glycoprotein multidrug transporter: Sensitivity of tryptophan residues to binding of drugs and nucleotides, *Biochemistry 39*, 14927−14938.
46. Dale, R. E., Eisinger, J., and Blumberg, W. E. (1979) The orientational freedom of molecular probes. The orientation factor in intramolecular energy transfer, *Biophys. J. 26*, 161−193.
47. Sawyer, W. H., Chan, R. Y. S., Eccleston, J. F., Davidson, B. E., Samat, S. A., and Yan, Y. L. (2000) Distances between DNA and ATP binding sites in the TyrR-DNA complex, *Biochemistry 39*, 5653−5661.
48. Shapiro, A. B., and Ling, V. (1998) Transport of LDS-751 from the cytoplasmic leaflet of the plasma membrane by the rhodamine-123-selective site of P-glycoprotein, *Eur. J. Biochem. 254*, 181−188.
49. Qu, Q., Russell, P. L., and Sharom, F. J. (2003) Stoichiometry and affinity of nucleotide binding to P-glycoprotein during the catalytic cycle, *Biochemistry 42*, 1170−1177.
50. Selvin, P. R. (1995) Fluorescence resonance energy transfer, *Methods Enzymol. 246*, 300−334.
51. Jones, P. M., and George, A. M. (1999) Subunit interactions in ABC transporters: Towards a functional architecture, *FEMS Microbiol. Lett. 179*, 187−202.
52. Jones, P. M., and George, A. M. (2004) The ABC transporter structure and mechanism: Perspectives on recent research, *Cell. Mol. Life Sci. 61*, 682−699.
53. Wang, E. J., Barecki-Roach, M., and Johnson, W. W. (2002) Elevation of P-glycoprotein function by a catechin in green tea, *Biochem. Biophys. Res. Commun. 297*, 412−418.
54. Shapiro, A. B., Corder, A. B., and Ling, V. (1997) P-Glycoprotein-mediated Hoechst 33342 transport out of the lipid bilayer, *Eur. J. Biochem. 250*, 115−121.
55. Sharom, F. J., Yu, X., Chu, J. W. K., and Doige, C. A. (1995) Characterization of the ATPase activity of P-glycoprotein from multidrug-resistant Chinese hamster ovary cells, *Biochem. J. 308*, 381−390.
56. Loo, T. W., and Clarke, D. M. (1997) Identification of residues in the drug-binding site of human P-glycoprotein using a thiol-reactive substrate, *J. Biol. Chem. 272*, 31945−31948.
57. Loo, T. W., and Clarke, D. M. (1997) Drug-stimulated ATPase activity of human P-glycoprotein requires movement between transmembrane segments 6 and 12, *J. Biol. Chem. 272*, 20986−20989.
58. Loo, T. W., and Clarke, D. M. (2002) Location of the rhodamine-binding site in the human multidrug resistance P-glycoprotein, *J. Biol. Chem. 277*, 44332−44338.
59. Romsicki, Y., and Sharom, F. J. (1999) The membrane lipid environment modulates drug interactions with the P-glycoprotein multidrug transporter, *Biochemistry 38*, 6887−6896.
60. Qu, Q., Chu, J. W., and Sharom, F. J. (2003) Transition state P-glycoprotein binds drugs and modulators with unchanged affinity, suggesting a concerted transport mechanism, *Biochemistry 42*, 1345−1353.
61. Kast, C., Canfield, V., Levenson, R., and Gros, P. (1996) Transmembrane organization of mouse P-glycoprotein determined by epitope insertion and immunofluorescence, *J. Biol. Chem. 271*, 9240−9248.
62. Sauna, Z. E., Smith, M. M., Müller, M., Kerr, K. M., and Ambudkar, S. V. (2001) The mechanism of action of multidrug-resistance-linked P-glycoprotein, *J. Bioenerg. Biomembr. 33*, 481−491.
63. Hopfner, K. P., Karcher, A., Shin, D. S., Craig, L., Arthur, L. M., Carney, J. P., and Tainer, J. A. (2000) Structural biology of Rad50 ATPase: ATP-driven conformational control in DNA double-strand break repair and the ABC-ATPase superfamily, *Cell 101*, 789−800.
64. Locher, K. P., Lee, A. T., and Rees, D. C. (2002) The *E. coli* BtuCD structure: A framework for ABC transporter architecture and mechanism, *Science 296*, 1091−1098.
65. Loo, T. W., Bartlett, M. C., and Clarke, D. M. (2003) Drug binding in human P-glycoprotein causes conformational changes in both nucleotide-binding domains, *J. Biol. Chem. 278*, 1575−1578.
66. Stryer, L. (1978) Fluorescence energy transfer as a spectroscopic ruler, *Annu. Rev. Biochem. 47*, 819−846.
67. Rosenberg, M. F., Mao, Q. C., Holzenburg, A., Ford, R. C., Deeley, R. G., and Cole, S. P. C. (2001) The structure of the multidrug resistance protein 1 (MRP1/ABCC1): Crystallization and single-particle analysis, *J. Biol. Chem. 276*, 16076−16082.
68. Seigneuret, M., and Garnier-Suillerot, A. (2003) A structural model for the open conformation of the *mdr1* P-glycoprotein based on the MsbA crystal structure, *J. Biol. Chem. 278*, 30115−30124.
69. Shapiro, A. B., and Ling, V. (1997) Extraction of Hoechst 33342 from the cytoplasmic leaflet of the plasma membrane by P-glycoprotein, *Eur. J. Biochem. 250*, 122−129.
70. Rosenberg, M. F., Callaghan, R., Ford, R. C., and Higgins, C. F. (1997) Structure of the multidrug resistance P-glycoprotein to 2.5 nm resolution determined by electron microscopy and image analysis, *J. Biol. Chem. 272*, 10685−10694.
71. Lee, J. Y., Urbatsch, I. L., Senior, A. E., and Wilkens, S. (2002) Projection structure of P-glycoprotein by electron microscopy: Evidence for a closed conformation of the nucleotide binding domains, *J. Biol. Chem. 277*, 40125−40131.

BI0485326